PHYSICAL REVIEW B VOLUME 32, NUMBER 8 15 OCTOBER 1985

Raman resonance on E_1 edges in superlattices

C. Tejedor, J. M. Calleja, and F. Meseguer
Departamento de Física and Instituto de Física del Estado Sólido, Universidad Autónoma de Madrid, Cantoblanco, 28049 Madrid, Spain

E. E. Mendez, C.-A. Chang, and L. Esaki
IBM Thomas J. Watson Research Center, Yorktown Heights, New York 10598
(Received 18 December 1984)

Resonant Raman scattering is used to study the electronic structure of GaSb-AlSb superlattices associated with E_1 transitions in GaSb. A new tight-binding approach is developed to analyze the experimental information. The properties of the resonance detected indicate a type-I superlattice at the L point that is consistent with a valence-band offset higher than 0.2 eV. Our results suggest that in our samples the lattice constant of AlSb is compressed to that of GaSb. The behavior of the resonances with temperature has been analyzed and indicates the detection of an interference of the allowed and forbidden mechanisms. We compare our results with previous experimental information.

I. INTRODUCTION

The study of artificial superlattices (SL's) has become one of the most active fields in the physics of semiconductors. Extensive information exists on systems like GaAs-$Ga_{1-x}Al_xAs$.[1] The interest is growing on more complicated SL's such as GaSb-AlSb where there is a small but significant lattice-constant mismatch (0.65%). In spite of the incommensurability of the lattices, GaSb-AlSb SL's have been grown by means of molecular-beam epitaxy.[2–4] The analysis of the samples by x-ray diffraction confirms both the periodicity of the structures and the crystalline quality of these SL's.[3] The main consequence of the lattice mismatch is the existence of strains in every component of the SL to make possible a perfect network. From the point of view of the electronic states, such strains perturb the bulk structure of the host materials producing important effects on the properties of the SL. The electronic structure of GaSb-AlSb SL's has been analyzed by electroreflectance,[3] luminescence,[3,4] and optical absorption,[5–7] showing unambiguously the formation of electronic subbands at the Γ point. However, it is not so easy to get information on the electronic states away from the center of the Brillouin zone. In this case, electroreflectance is the most successful technique used in other SL's.[8] The only published[3] electroreflectance spectrum of GaSb-AlSb shows four features. In this work[3] it is proposed that two of these features are associated with E_1 and $E_1+\Delta_1$ transitions in GaSb and the other two with E_0 and E_1 transitions in AlSb. However, there is not any clear evidence in support of such a proposal. Therefore, the aim of this paper is to perform a detailed analysis of the electronic structure of a GaSb-AlSb SL in the region of the Brillouin zone surrounding the L point of the zinc-blende structure. Due to practical reasons discussed below, we will concentrate on the feature that appears in the electroreflectance[3] spectra at room temperature at 2.16 eV in order to examine its possible connection with an E_1 transition in GaSb, as was proposed in Ref. 3. This requires an experimental technique able to detect which is the host semiconductor where the transition takes place. Resonant Raman scattering (RRS) fulfills this requirement because one can study the resonance spectra either of GaSb or AlSb optical phonons as a function of the laser frequency ω_L. Such resonance is connected with a transition between electronic states. Moreover, optical phonons are not significantly affected by the periodicity of the SL and they remain localized in the spatial region of the corresponding host semiconductor. Therefore the analysis of the resonance of an optical phonon of one of the semiconductors (GaSb in our case) gives us information about electronic transitions occurring in the spatial region of that semiconductor. To our knowledge this is the first time that RRS has been used in the study of the electronic structure of a SL away from the center of the Brillouin zone. The confidence in the ability of that technique for such a purpose is derived from the excellent results that it has given when applied to the study of electronic states of bulk semiconductors as well as those at the Γ point of GaAs-$Ga_{1-x}Al_xAs$ SL's.[9–12] On the other hand, since two different physical mechanisms are responsible for RRS, we will analyze the resonance for different configurations of the polarization of the incoming and scattered light in order to separate both contributions. We are working with E_1-type transitions well above the first optical gap. Then allowed (deformation-potential plus electro-optic) and forbidden (Fröhlich) scatterings are comparable in intensity, allowing us to detect the interference between them under suitable conditions.[13] This is the first time that the interference has been found in SL's. In previous cases[12] it was not found because the measurements were done around E_0-type transitions where forbidden scattering is clearly dominant and the interference is too small.[12] Moreover, the existence of interference gives us insight about the origin of the Fröhlich scattering in our samples.

A simple Kronig-Penney model only gives a qualitative understanding mainly due to complications produced by the lattice mismatch and to the fact that we are not working with states at band edges. Therefore, in order to get information from the experimental results, we have developed a new tight-binding approach to the problem which allows us to deal with those problems in a simple way. So we get some interesting information on the ionic redistribution necessary to accommodate the lattices, as well as on the relative position of the bands of the two semiconductors usually represented by the valence-band offset $\Delta E_v = E_v(\text{GaSb}) - E_v(\text{AlSb})$.

In Sec. II the experiments are presented. Section III is devoted to the theoretical model. Finally, in Sec. IV we discuss our experimental and theoretical results in order to obtain physical information which can be compared with that obtained in previous works.

II. EXPERIMENT

We have analyzed two GaSb-AlSb SL's of high purity ($N_A - N_D \approx 10^{15}$ cm^{-3}) grown on GaSb(001) substrates. The first SL, labeled 26-20, has 65 periods, each containing 26 monolayers of GaSb (≈ 80 Å) and 20 of AlSb (≈ 60 Å). The second SL, labeled 52-20, has 45 periods, each with 52 monolayers of GaSb (≈ 160 Å) and 20 of AlSb (≈ 60 Å). Periodicity and crystalline quality were confirmed by x-ray diffraction.[3] For comparison, a third sample of (001)-oriented bulk GaSb was studied as well. Measurements were performed between 4 and 300 K in a continuous-flux cryostat. All the Raman spectra were taken in the backscattering configuration on the (001) epitaxial surface. A tunable cw dye laser pumped by an Ar-ion laser was the source of excitation. Available dyes were rhodamine-110 and -6G, allowing us to get ω_L in the range between 2.12 and 2.30 eV. This restricted, us to the study of the electronic structure connected with E_1 in GaSb, as mentioned in Sec. I. In order to study the possible scattering mechanisms, spectra were taken in different polarization configurations. So, in the $z(xy)\bar{z}$ configuration, with $z \| (001)$ perpendicular to the layers, and $x \| (100)$ and $y \| (010)$, only allowed (a), deformation-potential plus electrooptic scattering appeared, while for $z(xx)\bar{z}$ only the forbidden Fröhlich interaction (R_F) was present. When the interference of both mechanisms was the aim of the measurement, the configurations $z(y'y')\bar{z}$ [$y' \| (110)$] and $z(x'x')\bar{z}$ [$x' \| (1\bar{1}0)$] were used to get information on $|R_F + a|$ and $|R_F - a|$.[13] In our backscattering configuration the spectrum shows only two features of interest: the peak corresponding to the LD phonon of GaSb and that corresponding to the LO phonon of AlSb. We have measured the intensity of these peaks as a function of ω_L. The data were normalized to the Raman intensity of a CaF_2 standard in order to correct them for the response function of the optical system and for the ω^4 law of the Raman cross section.

In the range of frequencies we used, the LO phonon of AlSb does not show any clear resonance, in contrast with the phonon of GaSb, where a resonance is observed. This indicates that for those energies there are electronic transitions localized in the spatial region of GaSb. Figure 1

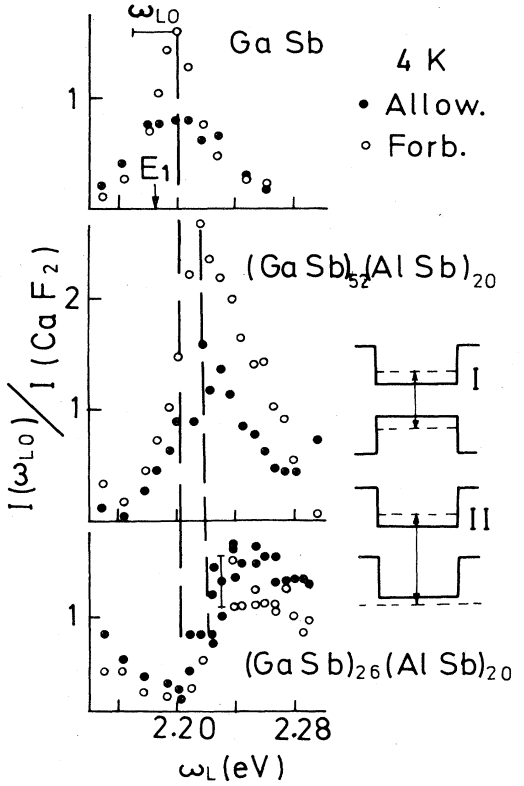

FIG. 1. Resonant Raman profiles for the LO phonon of GaSb in perfect GaSb and two different GaSb-AlSb SL's at 4 K. The results for allowed (●) and forbidden (○) scatterings are shown. The arrow in the upper part of the figure shows the position of the E_1 transition in GaSb measured by electroreflectance. Its shift with respect to the resonance is depicted by giving the LO-phonon frequency ω_{LO}. The inset shows the two possibilities for the SL transitions involved in the resonance (see text).

shows the resonant Raman profiles at 4 K for the LO phonon of GaSb in the three samples under study. In all cases there are clear resonances both for the allowed and forbidden mechanisms. They are much wider than the ones detected at the Γ point of the GaAs-$Ga_{1-x}Al_xAl$ SL.[11,12] This was expected because very narrow resonances are commonly associated with excitonic behavior typical of the band edges at the Γ point. The peaks shown in Fig. 1 are rather wide, being a mixture of both the incoming and outgoing resonances. This is supported by the fact, shown in Fig. 1, that in GaSb the resonance is shifted upwards by one-half of the phonon frequency (ω_{LO}) with respect to the E_1 transition measured by electroreflectance.[3] A similar behavior can be expected in SL's as will be checked later by comparing our Raman measurements at (RT) room temperature with the published electroreflectance data.[3] Then RRS gives direct information of the SL band structure. In our case the transition detected is associated with the E_1-type gap of GaSb, both by continuity of the peak position as a function of the SL period and because only the phonon of GaSb shows a resonance in this frequency region. The dependence of the resonance position on the SL period is

taken from Fig. 1, giving

$$\omega_{52\text{-}20}=\omega_{GaSb}+0.015 \text{ eV},$$

$$\omega_{26\text{-}20}=\omega_{GaSb}+0.055 \text{ eV}.$$

There is an important consequence derived not just from the existence and the intensity of the resonance but mainly from the dependence of its position on the well width. The transition connected with the resonance is localized in the GaSb region as mentioned before, but there are two reasonable possibilities, depicted in the inset of Fig. 1, for the states involved in that transition. Due to the differences in the band structures of both host semiconductors, the state at the conduction band is localized at GaSb and, as we shall see below, it does not shift significantly by changing the width of GaSb. However, the tops of the two valence bands at the L point are close enough to allow two possibilities for the SL valence state that is involved in the transition we are interested in. First, we could be seeing a type-I SL at the L point with a valence state localized in the GaSb region at energies that would depend on the width of the well. The second possibility is a type-II SL at the L point. In this case the state should leak into AlSb, considerably reducing the transition probability.[14] Even if this leak were small and the state remained essentially localized in GaSb, its energy should not depend significantly on the width of the well. The theoretical results shown in the next sections support these points. There, we have computed the SL eigenstates for different values of the valence-band offset ranging from type-II to type-I SL's at the L point. We have found that the upper valence states have a wave function with an extent which significantly depends on the type of SL. They are localized in GaSb for type-I SL's and very extended to AlSb for type-II SL's. Since our experimental results show a significant shift of the resonances as a function of the well width consistent with localization in GaSb, we claim that we are working with systems that are of type I at the L point.

Let us now analyze the temperature dependence of RRS in SL's, ω_{SL}. Figures 2 and 3 show resonant Raman profiles for the two SL's at 77 and 300 K, respectively. The 77-K case is rather similar to that of 4 K shown in Fig. 1, but the resonances are shifted to lower energies as it corresponds to a decrease of the gaps with increasing temperature. At RT two different behaviors are observed in Fig. 3. The allowed mechanism does not resonate any more, while forbidden scattering shows a resonance shifted to lower energies with respect to those found at low temperatures. The arrow included in the figure for the $(GaSb)_{26}(AlSb)_{20}$ SL shows the position of the electroreflectance feature attributed to a GaSb E_1 transition for that SL.[3] Once again the Raman resonance appears at a position roughly $\omega_{LO}/2$ higher than the electroreflectance value as it was observed in GaSb in Fig. 1. This confirms the assignment made in Ref. 3 as well as the ability of RRS to analyze the band structure of the SL. Figure 4 compiles all of our results. In order to clarify the dependence on temperature, the resonance of GaSb at RT (Ref. 15) is included to show that the variation of the ω_{SL} with temperature is slightly higher in GaSb than in our SL

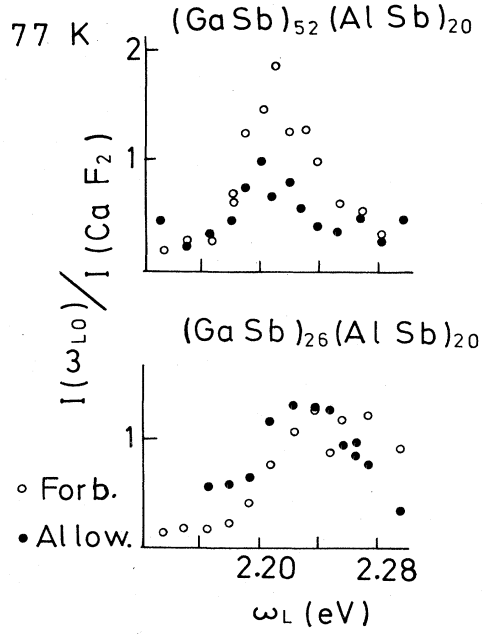

FIG. 2. Resonant Raman profiles for the LO phonon of GaSb in two different GaSb-AlSb SL's at 77 K. The results for allowed (●) and forbidden (○) scatterings are shown.

where $d\omega_{SL}/dT=-3.2\times10^{-4}$ eV K. This seems reasonable because the SL's have barriers of AlSb that always present temperature dependences smaller than those of GaSb.

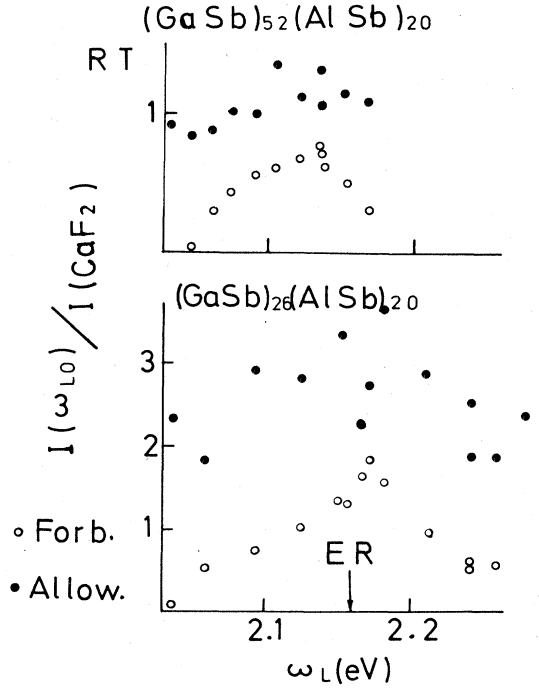

FIG. 3. Resonant Raman profiles for the LO phonon of GaSb-AlSb SL's at room temperature. The results for allowed (●) and forbidden (○) scatterings are shown. The arrow shows the position of the same feature measured by electroreflectance (Ref. 3).

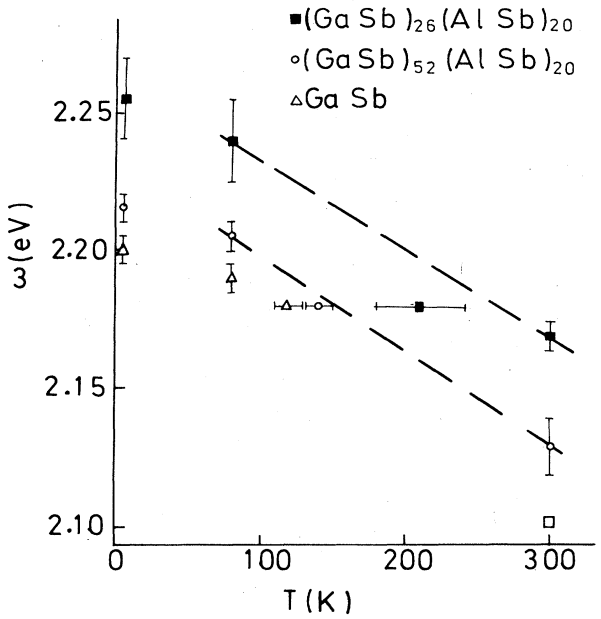

FIG. 4. Raman resonance peak position as a function of temperature for perfect GaSb and two different GaSb-AlSb SL's. The result for GaSb at RT (□) is taken from Ref. 15.

The comparison of the different behaviors of the allowed and forbidden scatterings with temperature is very suggestive. Let us concentrate on the $(GaSb)_{52}(AlSb)_{20}$ SL, where better profiles are obtained. At RT only the forbidden scattering resonates, being smaller in intensity over the whole frequency range than the allowed scattering. In contrast, at low temperatures both mechanisms do resonate, but now forbidden scattering has a higher intensity. The evident conclusion is that at intermediate temperatures it is possible to get a crossing of both mechanisms, i.e., the existence of interference at the appropriate configuration. Figure 5 shows clearly such interference

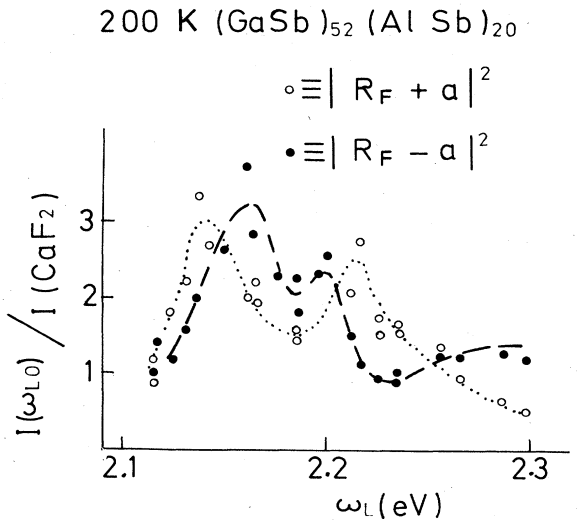

FIG. 5. Interference between (a) allowed and forbidden (R_F) scatterings in a $(GaSb)_{52}(AlSb)_{20}$ SL at 200 K. The lines are drawn as a guide to the eye.

displayed by the difference between the profiles of $|R_F+a|$ and $|R_F-a|$ obtained in $z(y'y')\bar{z}$ and $z(x'x')\bar{z}$ configurations. Two ingredients have contributed to the detection of the interference. The first is the tuning of temperature to get the desired relative values of the two mechanisms. The second is that we are working with transitions connected with the L point at frequencies significantly higher than the first optical transition. Therefore there is an important imaginary part of the allowed Raman tensor making possible the interference of both mechanisms. That is not the case for transitions close to E_0, where the interference becomes negligible.[12] The main consequence of the detection of the interference is that it implies the existence of coherence between allowed and forbidden scatterings.[13] This is a clear indication that Fröhlich scattering is not produced by impurities.[13] Instead it gives direct information of the band structure as, for instance, the value of $d\omega_{SL}/dT$ given above.

We have mentioned above the importance of temperature in the analysis of resonances. This temperature dependence could be used in a different way. Hitherto, temperature has been fixed so that the band structure of the system is determined. This band structure is analyzed by changing the frequency of the light. Another alternative should be to maintain the frequency of the light constant and vary the temperature so that the gaps could be tuned to the laser frequency. The results obtained by this procedure are shown in Fig. 6. They seem to be satisfactory mainly because of the interference shown in part (b) of the figure. However, when the results of part (a) of the figure are compared with those obtained for T fixed and ω_L variable, the agreement is rather poor. This is observed in Fig. 4, where the data for T variable are presented with the corresponding horizontal error bars. The data points deviate from the linear behavior of the previous experiment probably because the variation of temperature affects not only to the gap values, but also the electron-phonon interaction responsible for the resonance. Therefore this experiment does not seem to be a very good way to get information from RRS.

III. THEORETICAL MODEL

The analysis of the experimental results reported above requires the calculation of the SL band structure away from band edges at the center of the Brillouin zone. The use of a simple Kronig-Penney model is rather questionable, mainly when the existence of a lattice mismatch can distort the host semiconductors with respect to the perfect bulk ones. Then, two possibilities remain: the envelope-function approximation[16–18] or a tight-binding approach.[19,20] We think that the tight-binding approach is more appropriate because the small atomic displacements are very simply taken into account by scaling the Hamiltonian matrix elements as a function of the distance. The ingredients required are the following:

(i) Hamiltonian matrix elements in a localized basis: We used a nearest-neighbor approach in an sp^3s^* basis, which gives satisfactory results for the band structure of III-V semiconductors.[21] Spin-orbit interaction is included in this model Hamiltonian,[22] so that 20×20 matrices are

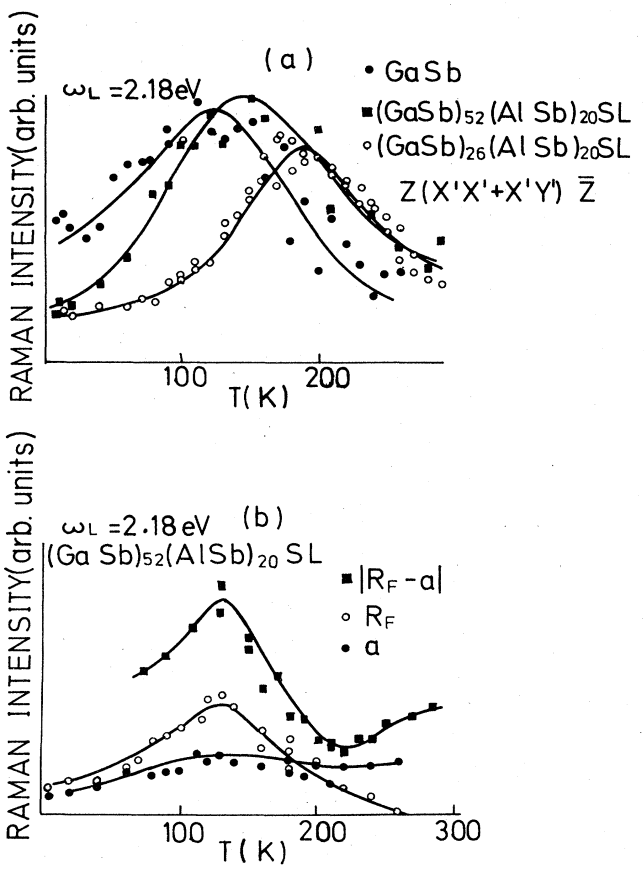

FIG. 6. Raman intensity of the LO mode of GaSb as a function of temperature for a given laser frequency ω_L. In part (a) we include the results for perfect GaSb and two different GaSb-AlSb SL's in a polarization where both allowed and forbidden scatterings are present. In part (b) we give the results for a $(GaSb)_{52}(AlSb)_{20}$ SL in three different configurations of the polarization in order to detect allowed (●), forbidden (○), or an interference (■) of these mechanisms, respectively.

required for zinc-blende semiconductors.

(ii) A scaling law for the Hamiltonian matrix elements: We use a d^{-2} law d being the interionic distance.[23,24]

(iii) The relative position of the band structure of the two host semiconductors: This is usually represented by the valence-band offset ΔE_v. We perform calculations for different values of this magnitude in order to get the optimum agreement with experimental results. In this way the experiments give information on the magnitude of this very important quantity. We will discuss this point more carefully later.

Once all these ingredients are chosen, the theoretical problem is completely determined. The practical difficulty remains the size of the matrices. In the case of a SL with m monolayers of one semiconductor and n of the other per unit cell, $20(m+n)\times 20(m+n)$ matrices are required. In actual problems like ours, this results in overly large matrices requiring highly-time-consuming computations with results that are difficult to interpret. Therefore we introduce a new method where only states in a given range of energies are included by means of a perturbative procedure. The advantages so obtained are the use of rather manageable matrices and the simple interpretation of the results in terms of the band structure of the host materials. The method is detailed in the Appendix, so that here we just sketch the idea. A $(GaSb)_m(AlSb)_n$ SL (or any other SL) can be considered as built up from a perfect GaSb (or AlSb) crystal with a supercell of size $m+n$ where n particular Ga ions are replaced by Al ions. The idea is to treat such replacement as a perturbation. The first step, a supercell with $m+n$ GaSb pairs of ions, is very easy to solve by the simple folding of eigenvalues and eigenvectors of the perfect semiconductors where only small matrices (20×20 in our case) must be solved. The second step of replacing n Ga ions by n Al ions is treated as a perturbation because of the similarity of the matrix Hamiltonians for perfect GaSb and AlSb. It is straightforward (see Appendix) to represent such a perturbation in the basis of the known folded eigenstates of GaSb. Since we are only interested in the states in a reduced range of energies, i.e., 3 or 4 eV, we can work only with a subbasis of the total basis of functions. In practical terms this means that typically we get any eigenstate of the SL as a combination of $m+n$, or less, eigenstates of one of the host semiconductors. In fact, we find that the SL states at the gap edges are a combination of only a few (≈ 5) states of the perfect semiconductor. As a test of the adequacy of this scheme we check that the results are quantitatively the same when starting either with GaSb or with AlSb in spite of the rather different gaps they have. The method has been tested by computing band structures of (GaAs)(AlAs) SL's where a lot of experimental[1] and theoretical[25] information exists. There the method yields results correct to the order of meV, which gives us confidence for using it in our present problem.

IV. DISCUSSION

Before discussing the results for the SL, some important information can be drawn from the band structure of the host semiconductors. The position of the conduction band at L with respect to the top of the valence band at Γ ($E_c^L - E_v^\Gamma$) is 0.88 eV in GaSb and 2.33 eV in AlSb. Since ΔE_v is of the order of a few tenths of an eV, that means that at the L-point electrons are localized in GaSb. It is not so clear for holes in the upper valence state at L. The difference between this level and the top of the valence band at Γ ($E_v^\Gamma - E_v^L$) is, in our calculation, 1.058 eV in GaSb and 0.791 eV in AlSb. Therefore for $\Delta E_v < 0.267$ eV we should have the holes at L in the AlSb region, i.e., a type-II SL, while for $\Delta E_v > 0.267$ eV we should have the holes at L in the GaSb, i.e., a type-I SL. By applying the theoretical method described in the preceding section we compute the wave functions of the SL states. We find that, for $\Delta E_v > 0.267$ eV, i.e., a type-I SL at L, both the lower conduction and the upper valence states are localized in GaSb. However, when $\Delta E_v < 0.267$ eV, i.e., a type-II SL at L, the upper valence states delocalize, leaking considerably into AlSb. Since our experimental results are consistent with localization on GaSb, it must be that $\Delta E_v > 0.267$ eV. This value is significantly higher than the $\Delta E_v \approx 0$ deduced from optical absorption in other

GaSb-AlSb SL's.[6,7] It must be pointed out that we have given the energy levels for perfect semiconductors. The appearance of strains to get a good lattice match tends to reduce energy differences in GaSb and increase them in AlSb.[5,15] This lowers the difference between GaSb and AlSb, requiring a smaller value of ΔE_v to get a type-I SL at L. Nevertheless, this effect is of the order of hundredths of an eV and ΔE_v must remain higher than 0.2 eV to get a type-I SL at L. Before comparing this conclusion with the different one of Voisin *et al.*,[6,7] it is convenient to present some of our other results. In our calculations the gaps at L do not change significantly if we vary ΔE_v from the minimum mentioned above up to 0.4 eV. They are more dependent on the rearrangement of the lattices at the SL. In general, our calculations give a difference between the gap at L in the SL and in GaSb which is smaller than the experimental shifts shown in Fig. 1. Therefore we get the best agreement by increasing the gaps in the SL as much as possible. The only way to do that is to increase the gaps of AlSb by compressing it to the GaSb lattice constant. There is one more argument supporting the compression of AlSb. If the lattice mismatch is accommodated by an expansion of GaSb, the position of the Raman resonance of GaSb would have an extra decrease in energy[15] and the difference between perfect GaSb and the SL should not be as big as the one shown in Fig. 1. Once again this conclusion is opposed to the GaSb strain proposed by Voisin *et al.*[6,7] However, we think that both results are not contradictory. The difference could be produced by the fact that in their samples both the substrate and the most abundant component of the SL is AlSb, so that it dominates in the determination of the lattice constant. However, in our samples, GaSb is the substrate and the most abundant component of the SL, so that the contrary should happen. This seems to be a reasonable explanation of the difference in lattice rearrangements. As far as the difference in ΔE_v is concerned, it is a consequence of the charge transfer between both semiconductors at each interface of the SL. This charge transfer is obviously affected by ionic positions.[25] These are different in our samples then in the ones used by Voisin *et al.*, so that it is possible that the values of ΔE_v are different too. In summary, the lattice mismatch is accommodated in different ways depending on the characteristics of the samples and causes of differences in the electronic structure.

Let us now proceed with a more detailed comparison between Raman resonances and theoretical results. Figure 7 shows experimental transitions at 4 K and SL eigenstates around band edges at L. Since our calculation gives the eigenfunctions, we have checked that the states presented in Fig. 7 are localized in the region of GaSb. The increase in the gap predicted by the theory is smaller than the shift of the resonance. A possible cause of disagreement could be that the tight-binding parameters are fitted to bands at Γ and X points, giving—at L—effective masses higher than the experimental ones. With smaller effective masses some improvement in the increases of the gaps could be obtained, but it should be too small to invoke it as the main source of disagreement. The disagreement is higher in the case of the 26-20 SL

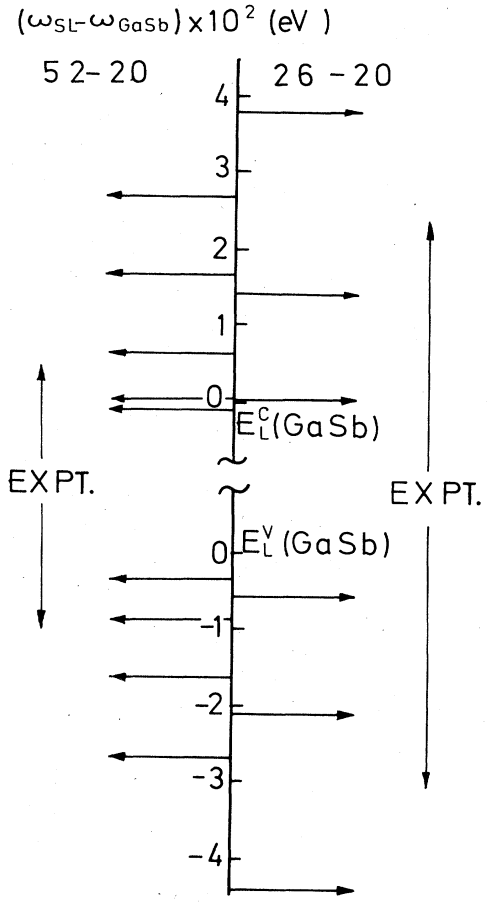

FIG. 7. Eigenstates around band edges at L for two different GaSb-AlSb SL's. Theoretical results are given with respect to the L-band edges of perfect GaSb because only relative energies are of interest. The experimental transitions detected by RRS are shown for comparison. Their location in the energy scale is arbitrary because only energy differences are experimentally available.

where the resonance has worse experimental resolution than the 52-20 SL. The width and asymmetry of the experimental resonances seem to indicate that several transitions can contribute to the resonance. This should significantly improve the agreement between theory and experiment. To check this point would require the computation of matrix elements and transition probabilities, which is beyond the scope of this paper.

An interesting fact to be noticed is that the lowest state of the SL conduction band does not shift practically from the one in GaSb. In fact, as can be seen in Fig. 7, for the 52-20 SL this state is even lower in energy than the one in GaSb. The reason is that since we are including spin-orbit interaction in the III-V compounds where no inversion center exists, the spin or Kramers degeneracy is broken, mainly along nonsymmetry directions as the one here analyzed, $(\frac{1}{2}\frac{1}{2}\frac{1}{2})+\lambda(001)$. Therefore when moving away from the L point the lowest conduction band moves down in energy. This becomes very important in the folding process induced by the SL formation, giving a conduction-band state at L that practically does not shift

for different widths of the well. A consequence of the stability of this L state is the possibility of having a Γ-L crossover because the conduction-band state at Γ of the SL moves up with respect to that of GaSb. In our model the shift of 70 meV of the Γ state required to get the crossover is obtained for well widths around 50 Å, in excellent agreement with experimental evidence.[4,7] This supports the conclusion that the shift of the resonance with the SL period indicates a type-I SL, because such a shift must be mainly due to the valence-band state at the GaSb region and this does not occur in a type-II SL, as was discussed before. Finally, it must be pointed out that the E_1 transition, and the corresponding Raman resonance of Fig. 1, comes not only from the L point, but from a region of the Brillouin zone around that point mainly along the Λ direction. We have applied our scheme to several of these points, obtaining results qualitatively similar to those presented here for L, thus reinforcing all our arguments.

In summary, by using RRS we have found resonances at the L point of GaSb-AlSb SL's. The behavior of the resonances with temperature has been analyzed, allowing the detection of an interference between allowed and forbidden scatterings which gives information about these mechanisms. The characteristics of the resonances indicate a type-I SL at L that would be consistent with a valence-band offset higher than 0.2 eV. Resonance position as a function of the well width indicates that AlSb is compressed in our samples to the lattice constant of GaSb. That is in contradiction to previous evidence, probably because of the different characteristics of the samples.

ACKNOWLEDGMENTS

This work has been supported in part by the Comisión Asesora para la Investigación Cientifica y Técnica of Spain, and by the U. S. Army Research Office. The Instituto de Física del Estado Sólido at the Universidad Autónoma de Madrid is supported by the Consejo Superiòr de Investigaciones Científicas.

APPENDIX

The tight-binding Hamiltonian H_{SL} for a $(\mathrm{GaSb})_m(\mathrm{AlSb})_n$ SL can be organized in blocks, each corresponding an atomic layer:

$$
\begin{array}{l}
(\mathrm{GaSb})_m \left\{ \vphantom{\begin{array}{c}1\\1\\1\\1\\1\\1\\1\\1\\1\end{array}} \right. \\
(\mathrm{AlSb})_n \left\{ \vphantom{\begin{array}{c}1\\1\\1\\1\\1\\1\\1\\1\end{array}} \right.
\end{array}
\begin{bmatrix}
\bar{A} & B^+ & & & & & & & & & & & & & d\eta^* \\
B & C & D^+ & & & & & & & & & & & & \\
 & D & A & B^+ & & & & & & & & & & & \\
 & & B & C & D^+ & & & & & & & & & & \\
 & & & & \ddots & & & & & & & & & & \\
 & & & & D & A & B^+ & & & & & & & & \\
 & & & & & B & C & D^+ & & & & & & & \\
 & & & & & & D & \bar{A} & b^+ & & & & & & \\
 & & & & & & & b & c & d^+ & & & & & \\
 & & & & & & & & d & a & b^+ & & & & \\
 & & & & & & & & & b & c & d^+ & & & \\
 & & & & & & & & & & & \ddots & & & \\
 & & & & & & & & & & & & d & a & b^+ \\
d^+\eta & & & & & & & & & & & & & b & c
\end{bmatrix} , \qquad \text{(A1)}
$$

where we have made use of the fact that both host semiconductors have the same anion. Each block has $\mathbf{k}$-dependent matrix elements between orbitals centered on anions $[A,a,\ \bar{A}=(A+a)/2]$, cations (C,c), or adjacent layers (B,D,b,d). Since we use an sp^3s^* basis including spin-orbit interaction, each block is a 10×10 matrix.[21,22] The wave vector also appears in the phase $\eta=\exp[i\pi(m+n)(k_z+k_y)]$ with the SL grown in the z direction. In order to get the eigenvalues and eigenvectors of H_{SL}, we decompose it as follows,

$$H_{\mathrm{SL}}=H_0+H_1 , \qquad \text{(A2)}$$

where

$$H_0=\begin{bmatrix} A & B^+ & & & & & D\eta^* \\ B & C & D^+ & & & & \\ & D & A & B^+ & & & \\ & & & \cdot & & & \\ & & & & \cdot & & \\ & & & & B & C & D^+ \\ & & & & D & A & B^+ \\ D^+\eta & & & & & B & C \end{bmatrix} \quad m+n \text{ rows} \tag{A3}$$

and

$$H_1=\begin{bmatrix} \overline{A}-A & & & & & & (d-D)\eta^* \\ & \overline{A}-A & b^+-B^+ & & & & \\ & b-B & c-C & d^+-D^+ & & & \\ & & & \cdot & & & \\ & & & & d-D & a-A & b^+-B^+ \\ (d^+-D^+)\eta & & & & & b-B & c-C \end{bmatrix} \Bigg\} (n) \text{ rows} . \tag{A4}$$

Equation (A2) between operators can be represented in the basis of eigenvectors of $H_0\{|i,\mathbf{k}\rangle\}$, where i is a band index. These states can be easily built up from the eigenstates of the 20×20 matrix describing the perfect GaSb crystal by the simple use of the Bloch theorem. In this way, only small matrices must be numerically solved. Then H_{SL} is a $20(m+n)\times20(m+n)$ matrix with elements

$$\langle i,\mathbf{k}\,|\,H_{\mathrm{SL}}\,|\,i'\mathbf{k}'\rangle=\epsilon_{i\mathbf{k}}\delta_{ii'}\delta(\mathbf{k}-\mathbf{k}')+\langle i\mathbf{k}\,|\,H_1\,|\,i'\mathbf{k}'\rangle\ , \tag{A5}$$

where ϵ_{ik} is given by diagonalization of the 20×20 matrix. The second term on the right-hand side of (A5) is straightforwardly obtained because H_1 is a sparse matrix. Moreover, this term is small because of the differences of matrices appearing in H_1. Therefore the secular equation for (A5) can be solved perturbatively. In other words, one can select a range of energies around the gap where the eigenstates of (A5) only have significant weight in a subbasis of $\{|i,\mathbf{k}\rangle\}$ with a dimension much smaller than $20(m+n)$.

The convergence of the method as a function of the dimension of the subbasis is easily tested by changing the whole procedure to make perturbation on AlSb instead of making it on GaSb. In general, good convergence is obtained when the dimension of the subbasis is of the order of $m+n$, which means a reduction of a factor of 20 with respect to the initial one. In this way one can manage actual SL's with a large number of atoms per unit cell.

[1]L. Esaki, in *Proceedings of the 17th International Conference on the Physics of Semiconductors,* edited by J. D. Chadi and W. A. Harrison (Springer-Verlag, New York, 1985).

[2]M. Naganuma, Y. Suzuki, and H. Okamoto, in *Proceedings of the Symposium on GaAs and Related Compounds* (IOP, Bristol, 1981), p. 125 (IOP Conf. Ser. No. 63).

[3]E. E. Mendez, C.-A. Chang, H. Takaoka, L. L. Chang, and L. Esaki, J. Vac. Sci. Technol. B **1**, 152 (1983).

[4]G. Griffiths, K. Mohammed, S. Subbana, H. Kroemer, and J. Merz, Appl. Phys. Lett. **43**, 1059 (1983).

[5]P. Voisin, G. Bastard, M. Voos, E. E. Mendez, C.-A. Chang, L. L. Chang, and L. Esaki, J. Vac. Sci. Technol. B **1**, 409 (1983).

[6]P. Voisin, C. Delalande, M. Voos, L. L. Chang, A. Segmuller, C.-A. Chang, and L. Esaki, Phys. Rev. B **30**, 2276 (1984).

[7]P. Voisin, C. Delalande, G. Bastard, M. Voos, L. L. Chang, A. Segmuller, C.-A. Chang, and L. Esaki, in *Proceedings of the International Conference on Superlattices, Microstructures and Microdevices,* Urbana—Champaign, August, 1984 (unpublished).

[8]E. E. Mendez, L. L. Chang, G. Landgren, R. Ludeke, L. Esaki, and F. Pollak, Phys. Rev. Lett. **46**, 1230 (1981).

[9]P. Manuel, G. A. Sai-Halasz, L. L. Chang, C. -A. Chang, and L. Esaki, Phys. Rev. Lett. **37**, 1701 (1976).

[10]C. Colvard, R. Merlin, M. V. Klein, and A. C. Gossard, Phys. Rev. Lett. **45**, 298 (1980).

[11]J. E. Zucker, A. Pinczuk, D. S. Chemla, A. Gossard, and W. Wiegmann, Phys. Rev. Lett. **51**, 1293 (1983).

[12]J. E. Zucker, A. Pinczuk, D. S. Chemla, A. Gossard, and W. Wiegmann, Phys. Rev. B **29**, 7065 (1984).

[13]J. Menéndez and M. Cardona, Phys. Rev. Lett. **51**, 1297 (1983).

[14]P. Voisin, G. Bastard, and M. Voos, Phys. Rev. B **29**, 935 (1984).

[15]K. Aoki, A. K. Sood, H. Presting, and M. Cardona, Solid State Commun. **50**, 287 (1984).

[16]S. R. White and L. J. Sham, Phys. Rev. Lett. **27**, 879 (1981).

[17]G. Bastard, Phys. Rev. B **24**, 5693 (1981); **25**, 7584 (1982).

[18]M. Altarelli, Phys. Rev. B **28**, 842 (1983).

[19]G. A. Sai-Halasz, L. Esaki, and W. A. Harrison, Phys. Rev. B **18**, 2812 (1978).

[20]J. N. Schulman and T. C. McGill, Phys. Rev. B **19**, 6341 (1979).
[21]P. Vogl, H. P. Hjalmarson, and J. D. Dow, J. Phys. Chem. Solids **44**, 365 (1983).
[22]D. J. Chadi, Phys. Rev. B **16**, 790 (1977).
[23]W. Harrison, *Electronic Structure and the Properties of Solids* (Freeman, San Francisco, 1980).
[24]L. Brey, C. Tejedor, and J. A. Verges, Phys. Rev. B **29**, 6840 (1984).
[25]J. Sanchez-Dehesa and C. Tejedor, Phys. Rev. B **26**, 5824 (1982).